Journal of Hazardous Materials 186 (2011) 1392–1397

Contents lists available at ScienceDirect

Journal of Hazardous Materials

journal homepage: www.elsevier.com/locate/jhazmat

Complete oxidation of formaldehyde at ambient temperature over supported Pt/Fe_2O_3 catalysts prepared by colloid-deposition method

Nihong An, Qiushi Yu, Gang Liu, Suying Li, Mingjun Jia*, Wenxiang Zhang*

State Key Laboratory of Theoretical and Computational Chemistry, College of Chemistry, Jilin University, JieFang Road 2519, Changchun 130023, China

ARTICLE INFO

Article history:
Received 30 June 2010
Received in revised form 23 October 2010
Accepted 6 December 2010
Available online 13 December 2010

Keywords:
Platinum catalysts
Colloid deposition
Formaldehyde
Complete oxidation

ABSTRACT

The catalytic properties of iron oxide supported platinum catalysts (Pt/Fe_2O_3), prepared by a colloid deposition route, were investigated for the complete oxidation of formaldehyde. It is found that all the Pt/Fe_2O_3 catalysts calcined at different temperatures (200–500 °C) were active for the oxidation of formaldehyde. Among them, the catalysts calcined at lower temperatures (i.e., 200 and 300 °C) exhibited relatively high catalytic activity and stability, which could completely oxidize HCHO even at room temperature. Based on a variety of physical–chemical characterization results, it is proposed that the presence of suitable interaction between Pt particles and iron oxide supports, which is mainly in the form of Pt–O–Fe bonds, should play a positive role in determining the catalytic activity and stability of the supported Pt/Fe_2O_3 catalysts.

© 2010 Elsevier B.V. All rights reserved.

1. Introduction

Formaldehyde (HCHO) is regarded as the major indoor pollutant emitted from buildings, furnishing materials and consumer products. Great efforts have been made to reduce the indoor emission of HCHO for satisfying the stringent environmental regulations. As one of the most attractive approach, low-temperature catalytic oxidation of formaldehyde (HCHO) to CO_2 and H_2O has received considerable attention [1–13]. A variety of catalysts, such as transition metal oxides [12,13], composite oxides [1], and supported noble metals have been used for this process [2–11]. Among them, noble metal catalysts exhibited promising catalytic performance at relatively low reaction temperatures. For example, it was reported that HCHO could be completely oxidized below 100 °C over some supported noble metal catalysts, including Au/CeO_2 [7,8], $Pd–MnO_x/Al_2O_3$ and Pd/MnO_2 catalysts [9,10].

Recently, significant progresses on decreasing the reaction temperature of HCHO oxidation have been achieved over supported Pt catalysts [3–6,11]. For instance, Zhang et al. [3,4] reported that a highly active Pt/TiO_2 catalyst, prepared by impregnation method, could completely oxidize HCHO even at ambient temperature. Shen and co-workers [6] found that 100% conversion of HCHO could be achieved at room temperature over $Pt/MnO_x–CeO_2$ catalyst prepared by impregnation method. These results suggest that highly active supported Pt catalysts for HCHO oxidation could be obtained through suitable preparation strategy (e.g., preparation methods, supports, and pretreatment conditions).

Recently, colloid-deposition route has shown unusual advantages on preparing supported noble metal catalysts, since this method is possible to maximize catalytic activity of noble metal catalyst through control not only on the particle size of noble metal clusters but also on its interaction with metal oxide support. For instance, active and stable supported gold catalysts for low-temperature CO oxidation have been prepared by using a colloid-deposition process [14].

In our previous work, a series of supported Pt catalysts were obtained via a colloid deposition route, and interestingly, iron oxide supported Pt catalyst (Pt/Fe_2O_3) exhibited excellent catalytic activity and long-term stability for the complete oxidation of CO at ambient temperature [15]. With this background, we reported a comparative study on HCHO oxidation over the Pt/Fe_2O_3 catalysts calcined at different temperatures in the present work. The physical–chemical properties of the Pt/Fe_2O_3 catalysts were characterized by the X-ray diffraction (XRD), transmission electron microscopic (TEM), the thermo-gravimetric differential thermal analysis (TG-DTA), temperature programmed reduction by H_2 (H_2-TPR), and the X-ray photoelectron spectra (XPS), in order to build correlation with the catalytic performance of the catalysts.

2. Experimental

2.1. Catalyst preparation

The Pt/Fe_2O_3 catalysts were prepared by a colloid deposition method described elsewhere [15], while the Pt colloidal solution

* Corresponding authors. Tel.: +86 431 85155390; fax: +86 431 88499140.
E-mail addresses: jiamj@jlu.edu.cn (M. Jia), zhwenx@jlu.edu.cn (W. Zhang).

0304-3894/$ – see front matter © 2010 Elsevier B.V. All rights reserved.
doi:10.1016/j.jhazmat.2010.12.018

was prepared according to the literature procedure [16]. Typically, a glycol solution of NaOH (120 mL, 0.25 M) was added into a glycol solution of H_2PtCl_6 (100 mL, 2 g/100 mL) with stirring for 1 h to form a brown solution. The resulting colloidal solution can be obtained by heating the brown solution at 140 °C for 3 h under the protection of Ar.

The precursor of iron oxide support, $Fe(OH)_3$ precipitate, was obtained by precipitation method using $Fe(NO_3)_3$ as iron resource and Na_2CO_3 as precipitation agent. Then, the mixed solution of Pt colloid and $Fe(OH)_3$ was heated at 80 °C under stirring to achieve deposition process. The solid was isolated and washed thoroughly with distilled water. Finally, the product was dried at 100 °C and calcined at desired temperatures (200–500 °C) in a flow of 20% O_2/Ar to obtain the resulting supported Pt catalysts (Pt/Fe_2O_3-*T*), where *T* represents the calcination temperature. For all the catalysts, the Pt:Fe atomic ratio determined by ICP was about 1:100.

2.2. Catalyst characterization

The X-ray diffraction (XRD) analyses of the catalysts were carried out using a D/Max-rA X-ray diffractometer operated at 30 kV and 40 mA employing nickel-filtered Cu Kα radiation. Transmission electron microscopic (TEM) images were obtained using H8100-IV election microscopic operated at 200 kV. The thermo-gravimetric differential thermal analysis (TG-DTA) of the sample was conducted on a Rigaku Standard Model thermal analyzer (in air atmosphere, flow rate: 90 mL/min; heat rate: 10 °C/min). Temperature programmed reduction by H_2 (H_2-TPR) measurements were carried out using an adsorption instrument equipped with a TCD. The samples were loaded and pretreated with Ar at 100 °C for 30 min to remove the adsorbed carbonates and hydrates. The H_2-TPR experiment was performed under the mixture of 5% H_2 in N_2 flow (30 mL/min) over 20 mg of catalyst at a heating rate of 10 °C/min. The uptake amount during the reduction was measured by a thermal conductivity detector (TCD). The X-ray photoelectron spectra (XPS) measurements were carried out on an ESCALAB250 X-ray photoelectron spectrometer, using Al Kα radiation as the excitation source. The XPS spectra were corrected by adjusting the C 1s peak to a position of 284.6 eV.

2.3. Catalytic test

For the HCHO oxidation tests, the reactor was a quartz tube, at the middle of which 0.2 g (40–60 mesh) catalyst was packed. A thermocouple was placed in the middle of the catalyst bed for temperature measurement. The gas mixture containing HCHO 100–500 ppm and 20 vol.% O_2 balanced by N_2 was introduced as the reactants. Gaseous HCHO was generated by flowing N_2 coming from a mass-flow controller through paraformaldehyde in an incubator. Products and reactants were analyzed by Shimadzu GC-8A gas chromatograph equipped with TCD detector, and the catalytic activity of the Pt/Fe_2O_3 catalysts was evaluated by the conversion of formaldehyde to CO_2.

3. Results and discussion

3.1. Structural features of the catalysts

The XRD patterns of pure Fe_2O_3 support and various Pt/Fe_2O_3 catalysts calcined at different temperatures are shown in Fig. 1. For the Pt/Fe_2O_3 catalysts, the diffraction peaks, appeared at $2\theta = 24.1°$, 33.1°, 35.6°, 40.8°, 49.4°, 54.0°, 57.5°, 62.6°and 64.0°, could be associated with the presence of α-Fe_2O_3 phase. The fact that no characteristic peaks attributing to platinum species appeared in the XRD patterns suggests that Pt particles should be highly dispersed on the surface of support. Notably, the intensity of the diffraction

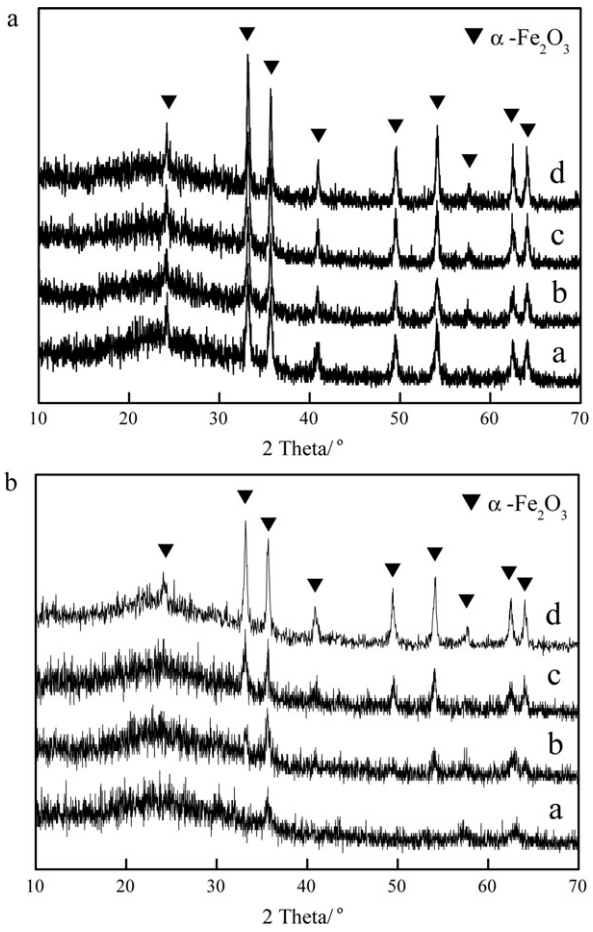

Fig. 1. XRD patterns of (a) pure iron oxide samples and (b) Pt/Fe_2O_3 catalysts calcined at different temperatures (a): 200 °C, (b): 300 °C, (c): 400 °C, and (d): 500 °C.

peaks of the iron oxide became stronger as the calcination temperature increased, indicating that the crystallinity of iron oxide increased gradually with calcination temperature. However, the diffraction peaks of iron oxide in Pt/Fe_2O_3 catalysts were much weaker than those of corresponded pure iron oxide (prepared by the same procedure just without introducing Pt species, see Fig. 1a). These results suggest that the existence of Pt particles on the surface of iron oxide could influence the crystallinity of iron oxide, implying that an interaction between Pt particles and iron oxide may be present in the Pt/Fe_2O_3 catalysts.

Fig. 2 shows the TEM images of Pt colloid, Pt/Fe_2O_3-200 catalyst and Pt/Fe_2O_3-500 catalyst. The Pt clusters in the native solution were uniform sphere with a small particle size and narrow size distribution (1.9 ± 0.3 nm). Depositing on the support, the size of the Pt particles in Pt/Fe_2O_3-200 had no obvious change in comparison with the colloidal Pt particles, and the Pt particles were homogeneously dispersed on the surface of iron oxide (Fig. 2c). Notably, no obvious aggregation of Pt particles occurred even when the catalyst was calcined at 500 °C (Pt/Fe_2O_3-500, see Fig. 2d), indicating the excellent stability of the Pt nanoparticles against thermal-sintering.

Thermal analysis results of as-prepared $Fe(OH)_3$ and the precursor of Pt/Fe_2O_3 catalyst (without calcination) are provided in Fig. 3. According to the TG curves, a weight loss existed in the whole process for both samples. For the $Fe(OH)_3$ sample, the DTA curve exhibited a endothermic peak at 110 °C and an exothermic peak at 420 °C, which could be assigned to dehydration process and the phase transformation of support, respectively. Compared with $Fe(OH)_3$, the DTA curve of the precursor of Pt/Fe_2O_3 catalyst showed an additional exothermic peak at around 200 °C, which can

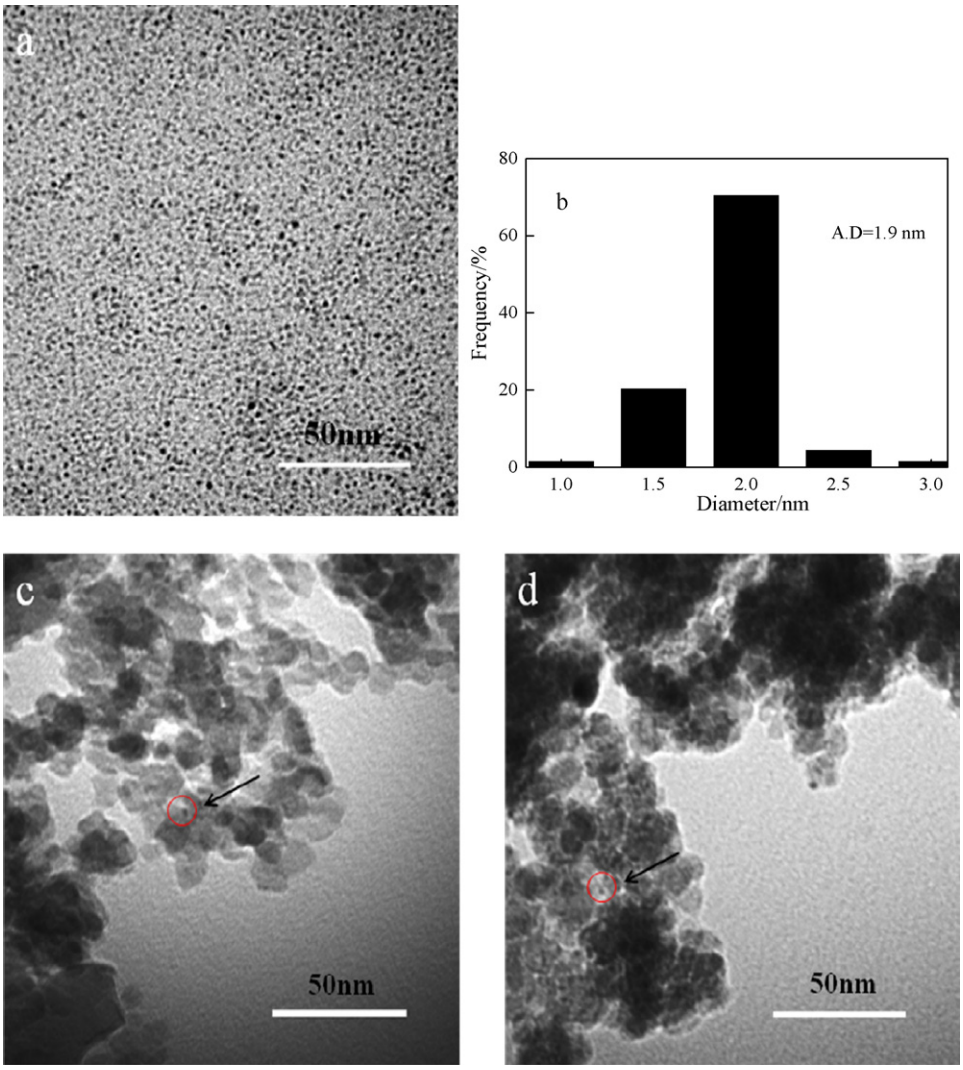

Fig. 2. TEM images of Pt colloid and supported Pt catalysts and Pt particle size distribution of Pt colloid: (a) Pt colloid; (b) Pt particle size distribution of Pt colloid; (c) Pt/Fe_2O_3-200; (d) Pt/Fe_2O_3-500.

be attributed to the decomposition or combustion of EG (ethylene glycol) in the sample. It is worth noting that the temperature for the phase transformation of support shifted to 620 °C when loading a certain amount of platinum on the support. These results suggest that the introduction of platinum species onto the surface of iron oxides could influence the nature and the growth of the iron oxides crystallites through an interaction between metal and support. A similar behavior has been reported by Chang et al. on the study of Au–Ru/Fe_2O_3 catalyst [17].

3.2. Catalytic activity

The catalytic activities of the Pt/Fe_2O_3 catalysts calcined at different temperatures were investigated in Fig. 4. Among them, Pt/Fe_2O_3-200 showed the highest catalytic activity toward the complete oxidation of HCHO. A 100% conversion of HCHO was achieved at a temperature as low as 25 °C. For the Pt/Fe_2O_3-300, Pt/Fe_2O_3-400 and Pt/Fe_2O_3-500 catalysts, complete conversion of HCHO was achieved at 35 °C, 40 °C and 60 °C, respectively. It should be mentioned here that, under the test conditions, pure Fe_2O_3 is inactive for the oxidation of HCHO to CO_2 even when the reaction temperature increased to 80 °C. Furthermore, it was found that the activity of Pt/Fe_2O_3-300 catalyst could be considerably improved by the addition of 3% water vapor into reactants, and the conversion of HCHO reached 100% at room temperature (data not shown in figure). This result suggests that the addition of a certain amount of water has a positive effect on the catalytic performance of Pt/Fe_2O_3-300 catalyst in HCHO oxidation at low temperature. In our previous work, a similar result has also been observed in the low-temperature CO oxidation over the supported Pt catalysts [15].

Fig. 5 shows the HCHO conversion with time-on-stream over Pt/Fe_2O_3-300 catalyst. It should be pointed out here that a 100% HCHO conversion could also be achieved on Pt/Fe_2O_3-300 catalyst at room temperature (without adding water), when a relatively low space velocity (i.e., 30,000 $cm^3/g\,h$) was adopted. Under the given reaction condition, HCHO could be oxidized completely for more than 360 h, indicating the excellent stability of the Pt/Fe_2O_3 catalyst. This result is much better than that of Pt/MnO_x–CeO_2 catalyst, which just could convert HCHO into CO_2 and H_2O completely for about 120 h at a similar operation condition, as reported in literature [6].

3.3. Redox and surface properties of the Pt catalysts

Fig. 6 compares XPS spectra of Pt 4f for various Pt/Fe_2O_3 catalysts calcined at different temperatures. The deconvolution of the Pt 4f photopeak provided three different contributions at 71.4–71.6 eV, 72.1–72.9 eV and 74.5–74.7 eV for these Pt/Fe_2O_3-CD catalysts. The

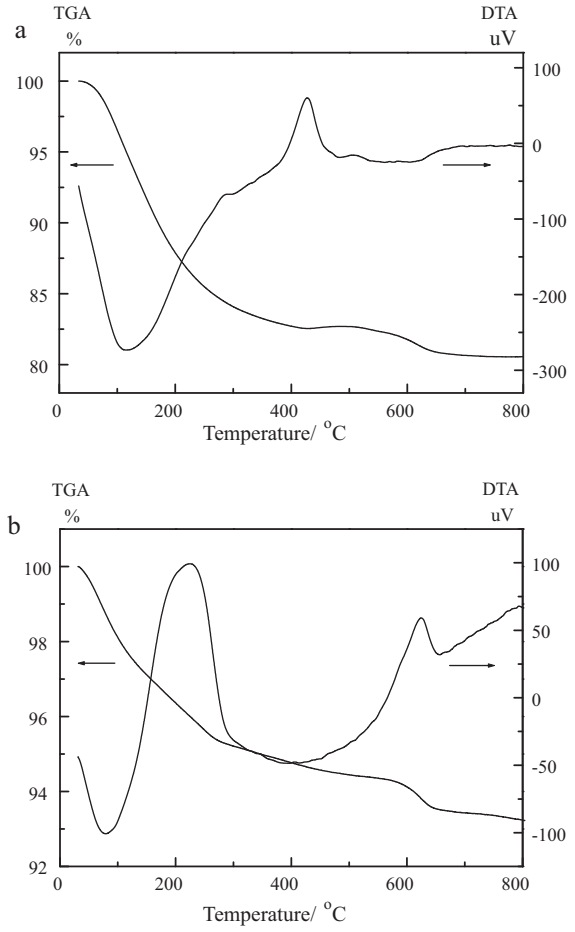

Fig. 3. TG-DTA analysis: (a) $Fe(OH)_3$; (b) the precursor of Pt/Fe_2O_3 catalyst (without calcination).

former BE value mainly characterized metallic Pt [18], whereas the latter two would correspond to Pt^{2+} and Pt^{4+}, respectively [19]. Table 1 shows the binding energies of Pt $4f_{7/2}$ as well as the relative surface concentrations of various Pt species for these Pt/Fe_2O_3 catalysts. The Pt $4f_{7/2}$ binding energies of Pt/Fe_2O_3-200 catalyst provided two different contributions with maxima at 71.4 eV and 72.7 eV, mainly characterizing Pt^0 and Pt^{2+}, respectively. For the Pt/Fe_2O_3-300 catalyst, coexistence of Pt^0, Pt^{2+} could be confirmed by the XPS spectrum. It was found that a higher proportion of

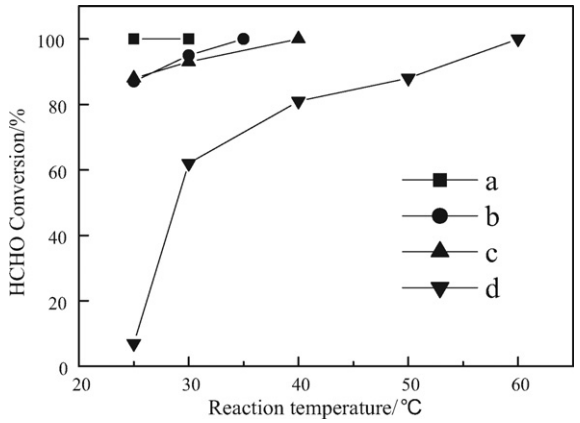

Fig. 4. Catalytic activity of the Pt/Fe_2O_3 catalysts calcined at different temperatures: (a) 200 °C; (b) 300 °C; (c) 400 °C; (d) 500 °C. Reaction conditions: HCHO 400 ppm, O_2 = 20 vol.%, N_2 balance, GHSV: 60,000 $cm^3/g\,h$.

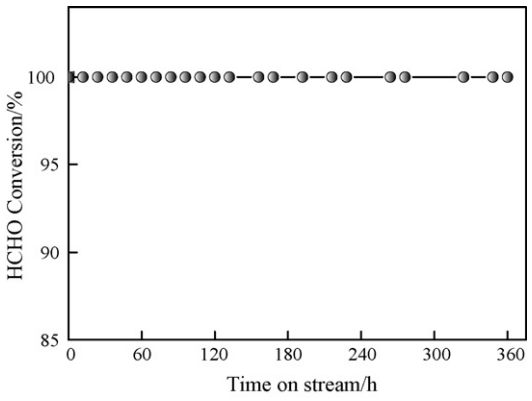

Fig. 5. Conversion of HCHO with time-on-stream over the 1% Pt/Fe_2O_3-300 catalyst. Reaction conditions: HCHO 200 ppm, O_2 20 vol.%, N_2 balance, GHSV: 30,000 $cm^3/g\,h$, reaction temperature: 25 °C.

Pt^{2+} was present on the Pt/Fe_2O_3-300 catalyst than that on the Pt/Fe_2O_3-200 catalyst. This result indicates that part of metallic state platinum could be oxidized to the platinum in higher valence states when increasing the calcination temperature. For the Pt/Fe_2O_3-400 catalyst, Pt $4f_{7/2}$ binding energies at 72.1 and 74.5 eV were due to Pt^{2+} and Pt^{4+}, while Pt^{2+} was the major species on this catalyst. With the further increase of calcination temperature, more highly oxidized Pt species (i.e., Pt^{4+}) were detectable in the Pt/Fe_2O_3-500 catalyst. Based on these results, it can be concluded that Pt/Fe_2O_3-CD-200 catalyst possesses the highest proportion of metallic Pt species, and the proportion of oxidized platinum species increases with improving the calcinations temperature.

The H_2-TPR profiles of the Pt/Fe_2O_3 catalysts calcined at different temperatures are shown in Fig. 7. In the TPR profiles of all the catalysts, the strong and broad reduction peak appeared around 600 °C was attributed to the transformation of Fe_3O_4 to FeO [17]. For the Pt/Fe_2O_3-200 catalyst, it exhibited an intensive low-temperature reduction peak at around 90 °C. The hydrogen consumption at this temperature was much greater than that necessary for the reduction of PtO_x, indicating that the partial reduction of the iron oxide, intimately contacted with Pt, should overlap with the reduction of PtO. The considerable decrease in the reduction temperature of iron oxide might be due to a certain amount of Pt oxide species have been introduced into iron oxide lattice in the form of Pt–O–Fe bonds, thus resulting in spillover of atomic hydrogen from Pt to the oxide surface occurs more easily. This result is consistent with the previous reports that the intimate contact between Pt and cerium in the $Pt/Ce–TiO_2$, Pt/CeO_2 catalysts facilitated the reducibility of the support at low temperatures [20–21]. As the calcination temperature up to 300 °C, the low-temperature reduction peak shifted slightly to a higher temperature region (around 105 °C), and an additional reduction peak appeared at about 270 °C which could be mainly attributed to the reduction of bulk Fe_2O_3. For the Pt/Fe_2O_3-400 and Pt/Fe_2O_3-500 catalysts, the intensity of the low-temperature reduction peak weakened gradually with the increase of calcination temperature. Meanwhile, two reduction peaks located at 220 °C and 270 °C could be clearly observed for the Pt/Fe_2O_3-400 catalyst. The former peak mainly characterized the reduction of oxidized Pt species (e.g., $Pt^{4+} \rightarrow Pt^0$) as the presence of Pt^{4+} species has been verified by the characterization results of XPS. The latter one would correspond to the reduction of bulk Fe_2O_3. Notably, the two reduction peaks integrated into single reduction peak with increasing the calcination temperature up to 500 °C. This reduction peak could be mainly ascribed to the reduction of crystalline Fe_2O_3, and may also include the reduction of PtO_x on the basis of XPS results and related literature [22].

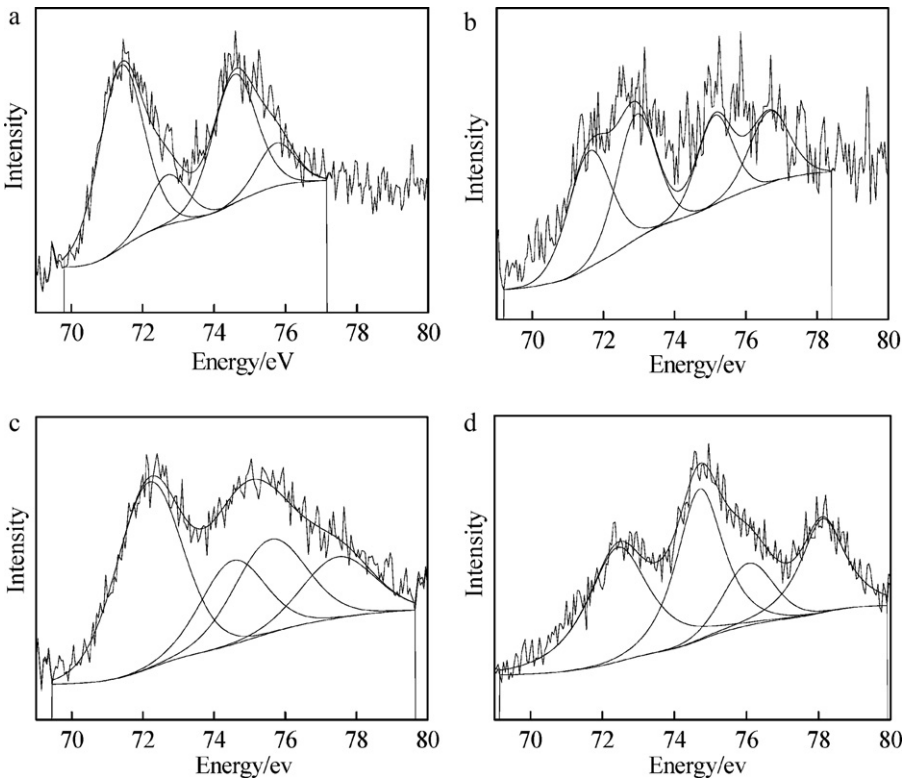

Fig. 6. XPS spectra of Pt 4f region for the 1%Pt/Fe_2O_3 catalysts calcined at varied temperatures: (a) 200 °C; (b) 300 °C; (c) 400 °C; (d) 500 °C.

Table 1
Summary of XPS data obtained for 1%Pt/Fe_2O_3 catalysts calcined at varied temperatures.

Catalyst	Species	Binding energy of Pt $4f_{7/2}$ (eV)	Relative intensity (%)
Pt/Fe_2O_3-200	Pt^0	71.4	80
	Pt^{2+}	72.7	20
Pt/Fe_2O_3-300	Pt^0	71.6	51
	Pt^{2+}	72.9	49
Pt/Fe_2O_3-400	Pt^{2+}	72.1	81
	Pt^{4+}	74.5	19
Pt/Fe_2O_3-500	Pt^{2+}	72.4	47
	Pt^{4+}	74.7	53

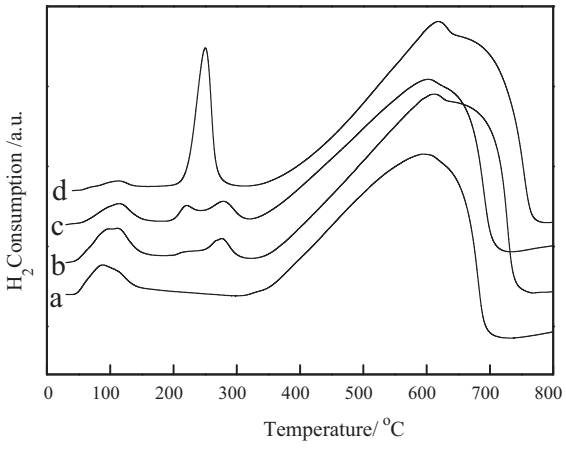

Fig. 7. H_2-TPR profiles of 1%Pt/Fe_2O_3 calcined at different temperatures: (a) 200 °C; (b) 300 °C; (c) 400 °C; (d) 500 °C.

Previously, it has been proposed that the proportion of Pt/PtO_x should be an important factor for influencing the activity of the supported Pt catalysts [23–25]. For instance, Gracia et al. [23] found that the catalytic activity of the supported Pt/Al_2O_3 catalyst could be closely correlated with the proportion of Pt/PtO_x, and fully oxidized Pt particles exhibit low activity for CO oxidation. Hong and coworkers [26] reported that the reduced Pt/TiO_2 catalysts displayed excellent activity in CO oxidation and the Pt species existed in the Pt^0 and Pt^{2+} states on these catalysts. In our case, the results of catalytic test showed that the catalysts of Pt/Fe_2O_3-200 and Pt/Fe_2O_3-300 possessed relatively high catalytic activity, while the XPS study revealed that both metallic Pt and oxidized Pt were present in these two catalysts. Hence, our results is in good agreement with the previous literatures, and provide a further evidence that the co-existence of metallic platinum and oxidized platinum species is preferable to enhance the catalytic activity of the platinum based catalysts [23–25,27].

It was generally known that Pt particle about 2 nm show high free energy and the equilibrium for oxidation is favored [28–30]. In our case, the co-existence of metallic platinum and oxidized platinum species in the relatively active and stable Pt/Fe_2O_3 catalysts may also be attributed to the presence of a suitable interaction between Pt particle and support (i.e., Pt–O–Fe), which can keep the Pt species in a stable chemical states and can also stabilize Pt particles against coalescence or sinter. In a recent work reported by Nagai et al. [31,32], they revealed that the presence of Pt–O–Ce bond in the Pt/CeO_2 catalyst could inhibit the sintering of Pt particles on the surface of oxide support, thus forming active and stable three-way catalyst. A similar interaction of Pt–O–Ce bonds was also reported for the high stability and activity of the Pt/CeO_2–Al_2O_3 catalyst and Pt/CeO_2 catalyst [18,33]. In present study, we suppose that the excellent low-temperature activity of Pt/Fe_2O_3 catalyst may be also partially assigned to the appearance of such kind of interaction. Through this Pt-oxide-support interaction, the redox property and the stability of Pt particles can be considerably influ-

enced. However, it should be pointed out here that other kind of Pt-support interaction can still be occurring, e.g., (Pt)n(PtOFe)m (adduct), Pt-Fe, which may also play important role for influencing the catalytic property of the supported Pt/Fe_2O_3 catalyst. Therefore, further work is still required in order to clarify the nature of the interaction between Pt particles and support, the physicochemical property of the active centers, as well as the mechanism of reaction.

4. Conclusions

Complete oxidation of HCHO at low temperature could be achieved over the iron oxide supported platinum catalysts prepared by a colloid deposition route. The catalysts of Pt/Fe_2O_3-200 and Pt/Fe_2O_3-300 exhibited relatively high catalytic activity and stability, which could completely oxidize HCHO even at room temperature. Physical–chemical analysis revealed that the Pt nanoparticles were well dispersed on the support and there was a relatively strong interaction between Pt and iron oxide support. The presence of a suitable interaction between Pt nanoparticles and iron oxide support could play positive role in influencing the physicochemical property as well as the catalytic performance of the Pt/Fe_2O_3 catalysts for low-temperature oxidation of HCHO.

Acknowledgement

This work was supported by the National Science Foundation of China (Grant No. 20973080).

References

[1] X. Tang, Y. Li, X. Huang, Y. Xu, H. Zhu, J. Wang, W. Shen, MnO_x–CeO_2 mixed oxide catalysts for complete oxidation of formaldehyde: effect of preparation method and calcination temperature, Appl. Catal. B: Environ. 62 (2006) 265–273.
[2] C. Li, Y. Shen, M. Jia, S. Sheng, M.O. Adebajo, H. Zhu, Catalytic combustion of formaldehyde on gold/iron-oxide catalysts, Catal. Commun. 9 (2008) 355–361.
[3] C. Zhang, H. He, K.-i. Tanaka, Catalytic performance and mechanism of a Pt/TiO_2 catalyst for the oxidation of formaldehyde at room temperature, Appl. Catal. B: Environ. 65 (2006) 37–43.
[4] C. Zhang, H. He, A comparative study of TiO_2 supported noble metal catalysts for the oxidation of formaldehyde at room temperature, Catal. Today 126 (2007) 345–350.
[5] J. Peng, S. Wang, Performance and characterization of supported metal catalysts for complete oxidation of formaldehyde at low temperatures, Appl. Catal. B: Environ. 73 (2007) 282–291.
[6] X. Tang, J. Chen, X. Huang, Y. Xu, W. Shen, Pt/MnO_x–CeO_2 catalysts for the complete oxidation of formaldehyde at ambient temperature, Appl. Catal. B Environ. 81 (2008) 115–121.
[7] Y. Shen, X. Yang, Y. Wang, Y. Zhang, H. Zhu, L. Gao, M. Jia, The states of gold species in CeO_2 supported gold catalyst for formaldehyde oxidation, Appl. Catal. B: Environ. 79 (2008) 142–148.
[8] J. Zhang, Y. Jin, C. Li, Y. Shen, L. Han, Z. Hu, X. Di, Z. Liu, Creation of three-dimensionally ordered macroporous Au/CeO_2 catalysts with controlled pore sizes and their enhanced catalytic performance for formaldehyde oxidation, Appl. Catal. B: Environ. 91 (2009) 11–20.
[9] M.C. Álvarez-Galván, V.A. de la Peña O'Shea, J.L.G. Fierro, P.L. Arias, Alumina-supported manganese and manganese–palladium oxide catalysts for VOCs combustion, Catal. Commun. 4 (2003) 223–228.
[10] M.C. Álvarez-Galván, B. Pawelec, V.A. de la Peña O'Shea, J.L.G. Fierro, P.L. Arias, Formaldehyde/methanol combustion on alumina-supported manganese–palladium oxide catalyst, Appl. Catal. B: Environ. 51 (2004) 83–91.
[11] R. Wang, J. Li, OMS-2 catalysts for formaldehyde oxidation: effects of Ce and Pt on Structure and performance of the catalysts, Catal. Lett. 131 (2009) 500–505.
[12] Y. Sekine, Oxidative decomposition of formaldehyde by metal oxides at room temperature, Atmos. Environ. 36 (2002) 5543–5547.
[13] Y. Sekine, A. Nishimura, Removal of formaldehyde from indoor air by passive type air cleaning materials, Atmos. Environ. 35 (2001) 2001–2007.
[14] M. Comotti, W.C. Li, B. Spliethoff, F. Schuth, Support effect in high activity gold catalysts for CO oxidation, J. Am. Chem. Soc. 128 (2005) 917–924.
[15] S. Li, G. Liu, H. Lian, M. Jia, G. Zhao, D. Jiang, W. Zhang, Low-temperature CO oxidation over supported Pt catalysts prepared by colloid-deposition method, Catal. Commun. 9 (2008) 1045–1049.
[16] Y. Wang, J. Ren, K. Deng, L. Gui, Y. Tang, Preparation of tractable platinum, rhodium, and ruthenium nanoclusters with small particle size in organic media, Chem. Mater. 12 (2000) 1622–1627.
[17] F.W. Chang, L.S. Roselin, T.C. Ou, Hydrogen production by partial oxidation of methanol over bimetallic Au–Ru/Fe_2O_3 catalysts, Appl. Catal. A: Gen. 334 (2008) 147–155.
[18] M. Hatanaka, N. Takahashi, N. Takahashi, T. Tanabe, Y. Nagai, A. Suda, H. Shinjoh, Reversible changes in the Pt oxidation state and nanostructure on a ceria-based supported Pt, J. Catal. 266 (2009) 182–190.
[19] J.P. Dacquin, M. Cabié, C.R. Henry, C. Lancelot, C. Dujardin, S.R. Raouf, P. Granger, Structural changes of nano-Pt particles during thermal ageing: support-induced effect and related impact on the catalytic performances, J. Catal. 270 (2010) 299–309.
[20] I.D. González, R.M. Navarro, W. Wen, N. Marinkovic, J.A. Rodriguéz, F. Rosa, J.L.G. Fierro, A comparative study of the water gas shift reaction over platinum catalysts supported on CeO_2, TiO_2 and Ce-modified TiO_2, Catal. Today 149 (2010) 372–379.
[21] N. Barrabés, K. Föttinger, J. Llorca, A. Dafinov, F. Medina, J. Sá, C. Hardacre, G.n. Rupprechter, Pretreatment Effect on Pt/CeO_2 Catalyst in the selective hydrodechlorination of trichloroethylene, J. Phys. Chem. C 114 (2010) 17675–17682.
[22] I.D. González, R.M. Navarro, M.C. Álvarez-Galván, F. Rosa, J.L.G. Fierro, Performance enhancement in the water–gas shift reaction of platinum deposited over a cerium-modified TiO_2 support, Catal. Commun. 9 (2008) 1759–1765.
[23] F.J. Gracia, J.T. Miller, A.J. Kropf, E.E. Wolf, Kinetics, FTIR, and controlled atmosphere EXAFS study of the effect of chlorine on pt-supported catalysts during oxidation reactions, J. Catal. 209 (2002) 8–354.
[24] F. Sen, G. Gokağac, Different sized platinum nanoparticles supported on carbon: an XPS study on these methanol oxidation catalysts, J. Phys. Chem. C 111 (2007) 5715–5720.
[25] P.L. Kuo, W.F. Chen, H.Y. Huang, I.C. Chang, S.A. Dai, Stabilizing effect of pseudo-dendritic polyethylenimine on platinum nanoparticles supported on carbon, J. Phys. Chem. B 110 (2006) 3071–3077.
[26] P.W. Seo, H.J. Choi, S.I. Hong, S.C. Hong, A study on the characteristics of CO oxidation at room temperature by metallic Pt, J. Hazard. Mater. 178 (2010) 917–925.
[27] R. Burch, P.K. Loader, Investigation of methane oxidation on Pt/Al_2O_3 catalysts under transient reaction conditions, Appl. Catal. A: Gen. 122 (1995) 169–190.
[28] Y. Tang, L. Zhang, Y. Wang, Y. Zhou, Y. Gao, C. Liu, W. Xing, T. Lu, Preparation of a carbon supported Pt catalyst using an improved organic sol method and its electrocatalytic activity for methanol oxidation, J. Power Sources 162 (2006) 124–131.
[29] F. Parmigiani, E. Kay, P.S. Bagus, Anomalous oxidation of platinum clusters studied by X-ray photoelectron spectroscopy, J. Electron. Spectrosc. Relat. Phenom. 50 (1990) 39–46.
[30] Y. Takasu, Y. Fujii, K. Yasuda, Y. Iwanaga, Y. Matsuda, Electrocatalytic properties of ultrafine platinum particles for hydrogen electrode reaction in an aqueous solution of sulfuric acid, Electrochim. Acta 34 (1989) 453–458.
[31] Y. Nagai, T. Hirabayashi, K. Dohmae, N. Takagi, T. Minami, H. Shinjoh, S.i. Matsumoto, Sintering inhibition mechanism of platinum supported on ceria-based oxide and Pt-oxide-support interaction, J. Catal. 242 (2006) 103–109.
[32] Y. Nagai, K. Dohmae, Y. Ikeda, N. Takagi, T. Tanabe, N. Hara, G. Guilera, S. Pascarelli, M.A. Newton, O. Kuno, H. Jiang, H. Shinjoh, S.i. Matsumoto, In situ redispersion of platinum autoexhaust catalysts: an on-line approach to increasing catalyst lifetimes, Angew. Chem. Int. Ed. 47 (2008) 9303–9306.
[33] A.P. Ferreira, D. Zanchet, J.C.S. Araújo, J.W.C. Liberatori, E.F. Souza-Aguiar, F.B. Noronha, J.M.C. Bueno, The effects of CeO_2 on the activity and stability of Pt supported catalysts for methane reforming, as addressed by in situ temperature resolved XAFS and TEM analysis, J. Catal. 263 (2009) 335–344.